REFERENCES

1. A. Zenasni et al, J. Appl. Phys. **102** (9) (2007).
2. M. Aimadeddine et al. in *Robust integration of an ULK SiOCH dielectric (k=2.3) for high performance 32nm node BEOL* (International Interconnect Technology Conference, 2007) pp. 175-177.
3. O. Gourhant et al. in *Extendibility of the PECVD Porogen Approach for ULK Materials*, (Mater. Res. Soc. Symp. Proc. **990**, San Francisco, CA, 2007) pp. 45–50.
4. D. R. Anderson, *Analysis of Silicones, chapter 10* (Willey-Interscience, NY, 1974).
5. S. P. Mukherjee et al., Thin Solid Films **14**, 105 (1972).
6. V. Jousseaume et al., J. Electrochem. Soc. **154** (5), G103 (2007).
7. P. Gonon et al, J. Electrochem. Soc., **150** (3), F47 (2003).

Conference Proceedings AMC XXIV © 2009 Materials Research Society

Engineering of Chemical and Physical Properties of Low-k Materials by Different Wavelength of UV Light

Premysl Marsik[1,2], Adam Urbanowicz[1], Patrick Verdonck[1], Karim Ferchichi[1], David DeRoest[3], Lutz Prager[4], and Mikhail R Baklanov[1*]
1AMPS, IMEC, Kapeldreef 75, Leuven, 3001, Belgium
2UFKL, Masaryk University, Kotlarska 2, Brno, 61137, Czech Republic
3ASM Belgium, Kapeldreef 75, Leuven, 3001, Belgiim
4 Leibniz-Institut für Oberflächenmodifizierung, Permoserstrasse 15, 04318 Leipzig, Germany
* corresponding author: baklanov@imec.be

ABSTRACT

SiCOH low-k films were deposited by PECVD with variable flow rates of porogen and matrix precursors and variable substrate temperature and RF power. Two precursor ratios were chosen leading to 1) material with higher target porosity around 33% and target k-value 2.3 and 2) material with lower porosity around 25% and target k-value 2.5. After deposition, the samples were UV-cured on temperature above 400°C in nitrogen ambient. Two types of curing lamps were used for the experiments: 1) lamps "A" emitting photons with energies higher than 6.5 eV (λ<190 nm) and 2) lamps "B" with photon energies below 6.2 eV (λ>200 nm). For all properties evaluated, irradiation at wavelengths below 190 nm resulted in more pronounced changes than at longer wavelengths. Lamps A provide fast decrease of porogen content, conversion of the Si–O–Si bonds from cage to network. However, degradation of Si–CH_3 bonds is significant, as well as formation of H–SiO (Si-H) bonds and amorphous carbon like porogen residue. Lamps B provide more slow porogen removal, do not decrease Si-CH_3 concentration and leave less porogen residues. Application of UV ellipsometry (138 nm -165 nm) for the low- k films, pure matrix material and pure porogen allowed obtaining additional results important for discussions. These findings are well confirmed by quantum-chemical calculations.

INTRODUCTION

Porous low-k dielectric films are introduced as interconnect-dielectric in integrated circuits below 45nm technology node. The actual approach is PECVD co-deposition of SiCOH matrix from selected precursor together with sacrificial organic porogen [1]. The porogen is afterwards removed during annealing [2,3] or UV assisted cure [4]. The resulting material must contain porosity sufficient for lowering the dielectric constant (k) down to target values. The lowered density of the material leads to reduced mechanical properties. The material must be hydrophobic, otherwise the physisorbed water (k~80) in the pores interior deteriorates the k-value. For successful implementation of the porous low-k's into industrial processes, the chemical and plasma damage resistance must be understood and assured.

The UV assisted annealing (UV-cure) is being favored for efficient removal of the porogen in short time [5] and for the changes of the matrix material leading to improved mechanical properties [4,6]. The choice of UV-curing light source has been attracting the interest, because the photons with higher energies cause greater changes to the matrix, improving the mechanical properties, but also can break the Si-CH_3 bond resulting in replacement by Si-H or Si-OH, shrinkage and hydrophilicity [7,8]. The influences of porogen loading and deposition condition and its removal have been studied for annealing cures [3,9]. The purpose of our study is

to relate some of possible variables of the deposition and curing to the film compositional and structural properties.

EXPERIMENT

We deposited the low-k material as 200 nm films on Silicon (100) wafers in ASM Eagle 12 system using variable flow rates of porogen and matrix precursors and variable substrate temperature and RF power. Two precursor ratios were chosen leading to 1) material with higher target porosity around 33% and target k-value 2.3, denoted as "CVD1" in this paper and 2) material with lower porosity around 25% and target k-value 2.5 denoted as "CVD2". The deposition conditions were chosen as 1) higher substrate temperature (300°C) and higher RF power (1850 W – 1900 W), further denoted by abbreviation "Hi" and 2) lower temperature (250°C) and lower RF power (1400 W), denoted by abbreviation "Lo".

After deposition, the samples were treated by UV-cure on temperature above 400°C in nitrogen purged ambient. Two curing lamps were used for the experiment: 1) lamp "A" emitting photons with energies higher than 6.5 eV (λ<190 nm) and 2) lamp "B" with photon energies below 6.2 eV (λ>200 nm). For both lamps, two curing times were chosen. Shorter time "1" is a half of the longer time "2", which is set as curing time for standard process. Therefore we obtained 16 samples with variable properties. Only already cured samples were studied, however, the thickness was measured before and after UV-cure, allowing calculation of shrinkages of the film.

The optical response of the films has been measured in the range from 2 eV to 9 eV (wavelengths from 620 nm down to 138 nm) using a variable-angle of incidence spectroscopic ellipsometer Sopra GES5 PUV. This tool operates in the rotating analyzer and fixed polarizer configuration with quartz Rochon cubes used as the polarizers, deuterium discharge light source and photomultiplier detector. To achieve a high transmittance for ultraviolet photons, the tool is surrounded by a glove box purged by nitrogen, keeping the oxygen and water concentrations below 1 ppm. For all of the samples, we applied three angles of incidence: 60, 70 and 80 degrees.

The measured spectra of ellipsometric angles Ψ and Δ [10] were fitted by single layer optical model (substrate – layer – ambient) using Marquardt-Levenberg algorithm. The dielectric function ε of the low-k film was modeled by generalized Gauss-Lorentz (G-L) peaks, calculated as rational approximations [11]. The dielectric function ε is recalculated to refractive index n and extinction coefficient k for the reader's convenience.

The porosity measurements were performed on a prototype ellipsometric porosimeter EP10, equipped with a fixed angle of incidence (70 deg) ellipsometer Sentech 801, operating on wavelengths between 350 nm and 850 nm, mounted on a high vacuum chamber with controllable pressure of solvent vapors. The principle of ellipsometric porosimetry is based on pressure dependent adsorption of a fluid (in our case toluene) into the pores. The absorbed toluene modifies the optical properties of the porous sample in the means of effective media and the changes are measured by ellipsometry. The volume ratio of the open pores is then obtained [12].

The infrared absorption of the layers in the range 400-4000 cm^{-1} is measured by a Fourier-transformed infrared (FTIR) spectrophotometer Biorad QS2200 ME with 4 cm^{-1} spectral resolution. The optical response is evaluated as absorbance. The absorbance of the substrate Silicon wafer is subtracted and the resulting spectrum is treated by baseline subtraction and renormalization.

RESULTS AND DISCUSSIONS

Infrared absorbance

We measured the FTIR transmission spectra of the 16 samples and fitted the observed structures using multiple Gaussian peaks. The calculated integrals were normalized to the integral of SiO_2 band. The FTIR spectra show following features [2]: The porogen CH_x absorption band is observed around 2900 cm^{-1}, but the dominant peak at 2973 cm^{-1} is attributed to CH_3 and therefore shows also response from methyl groups bonded in the SiCOH matrix. The Si-CH_3 signature is pronounced well at 1275 cm^{-1} and the SiO_2 band is observed as double peak structure localized at 1130 cm^{-1} (cage) and 1050 cm^{-1} (network). The Si-H bond vibration is detected at 2240 cm^{-1} and 890 cm^{-1}. We observe presence of C=C bonds in all the samples as small band at 1600 cm^{-1}.

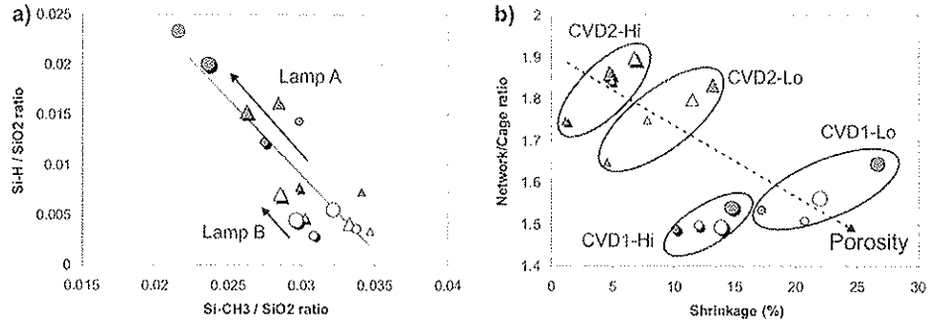

Figure 1 a) Anticorrelation of FTIR peaks related to SiH and $SiCH_3$ bond vibrations, normalized to peak area of SiO_2. The solid line represents the linear regression of the 16 points. **b)** Ratio of FTIR peaks related to SiO_2 network and cage versus the shrinkage of the samples. The dashed arrow follows the direction to higher porosities. - The triangles and circles refer to material CVD1 (higher porosity) resp. CVD2 (lower porosity). The symbols with shadow refer to higher deposition temperature and RF power ("Hi") and the flat symbols refer to lower deposition temperature and RF power ("Lo"). The color of the symbol denotes the curing lamp: Grey symbols for lamp A and white symbols for lamp B. Increasing symbol size denotes increasing curing time.

In figure 1a, we show the integral absorbance of the Si-CH_3 peak at 1275 cm^{-1} related to the integral absorbance of the Si-H peak at 890 cm^{-1}, both relative to the integrated absorption of SiO_2 band between 950 cm^{-1} and 1250 cm^{-1}. There is a strong anticorrelation between the Si-CH_3 peak and the Si-H peak. With increasing curing time, the Si-CH_3 presence is reduced and Si-H bonds are created through a process described in the literature [4,13]. This process is much stronger for the curing lamp A. The energy of the photons of the lamp A (7.2 eV) is sufficient to break the Si-CH_3 bond as expected from quantum-chemical calculations [8]. The experiments applying the UV cure with lamp A to the matrix material itself, without the porogen [14], resulted also in Si-CH_3 reduction, however, no Si-H creation was observed. This suggests that the porogen is the main source of hydrogen in this reaction.

Figure 1b shows ratio of the FTIR peaks assigned to network (around 1050cm^{-1}) and cage structure (around 1130 cm^{-1}) of the SiO_2 skeleton ("networking") compared to shrinkage of the film during the UV-cure. We observe the correlation between the "networking" and the shrinkage with increasing curing time, but this correlation occurs separately in the groups of the same material, deposited in given conditions. In all four groups, lamp A induces more changes than lamp B. Among the groups, this correlation is suppressed in spite of porosity: From material to material the porosity is the leading factor influencing the shrinkage and the "networking": 1) The samples with higher porosities show also higher shrinkage and 2) higher porosity is followed by lower network to cage ratio. It should be noticed that the link between shrinkage and the $SiCH_3$ reduction is also valid only within the groups of given material.

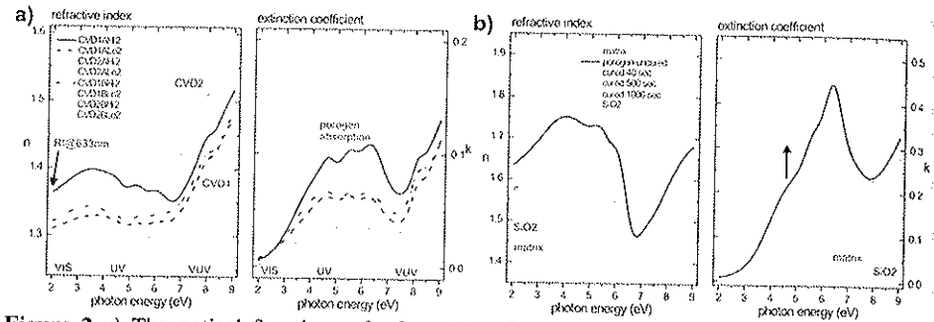

Figure 2 a) The optical functions of selected low-k samples. **b)** Optical functions of porogen films UV-cured for various curing times from 0 sec to 1000 sec and the optical functions of the matrix material. The properties of SiO_2 are plotted for comparison.

UV optical properties

The ultraviolet optical response of the low-k dielectric in the visible and ultraviolet range is determined by presence of porogen and its removal during the cure [15]. We determined the optical properties of the low-k films by spectroscopic ellipsometry and prepared and measured also samples of matrix material alone, without porogen and the organic porogen itself to be able to distinguish the impact of the both constituents. The refractive index and extinction coefficient of the low-k samples are plotted on the figure 2a and the properties of the constituents are plotted on figure 2b together with the properties of SiO_2 for comparison. The global "Cauchy-like" dispersion of the refractive index of the low-k films is following the same trend as the SiCOH matrix and SiO_2; in both cases the dispersion is given by strong absorption of SiO_2 above the measured range, while the porogen contributes to the absorption with the three peak structure between 4 eV and 7 eV in the extinction coefficient. These absorption bands produce the "s"-structure in the refractive index dispersion, shifting up its values in the visible range.

The evolution of the spectra of the low-k during the UV-cure follows the changes observed on the porogen samples and therefore we plotted only the samples with longer curing time in the figure 2a. The deposited porogen layer exposed to the UV light (lamp A in this case) shows fast shrinkage reduction (i.e. removal), but the layer is not removed completely (up to 80%) and the properties are changing [14]. The dominant absorption structure at 6.4 eV is suppressed in spite of growing band around 4.5 eV, followed by the growth of refractive index in

the visible ("RI"). In the spectra of the low-k samples, the main difference is observed between the CVD1 and the CVD2 material. The material CVD1 poses higher porosity and so the overall values of refractive index are lower (particularly observable above 7 eV) than the CVD2, however, it contains generally more porogen residues, observable as higher absorption between 4 eV to 7 eV. This absorption is transferred to refractive index as increased values on the lower energies (in the visible range). Therefore, the value of refractive index at 633nm ("RI") carries mixed information about the density of the material and the porogen residues.
As we described in [14], the knowledge of the properties of the constituents and the porosity percentage measured by ellipsometric porosimetry raises the possibility to estimate the volume percentages of the matrix and porogen residue as well, using the three media Bruggeman approximation [16].

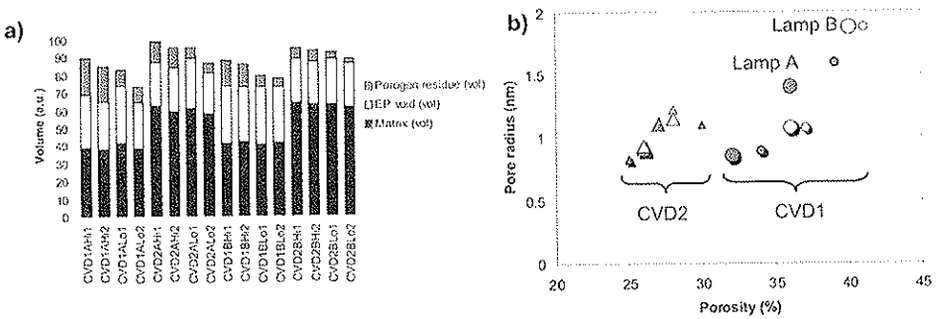

Figure 3 a) Estimated compositions of the samples recalculated to arbitrary volume using the measured shrinkage. **b)** The pore radius and the total open porosity of the samples measured by ellipsometric porosimetry with toluene. For the symbol description see caption of figure 1.

Figure 3a presents the results of estimation of the composition using the porosity measured by EP and the VIS/UV spectra (both refractive index and extinction coefficient). The results were obtained in the form of volume percentages and were recalculated to arbitrary volume quantities applying the measured shrinkage. Therefore, the total heights of the bars in the graph represent the relative thicknesses (i.e. volumes) of the samples and the three parts of the bar represent the individual constituents are in a comparable way. We observe basic difference between the matrix volumes of the material CVD1 (deposited with less matrix precursor and more porogen) and CVD2 (more matrix precursor, less porogen), while the volume of the matrix remains more or less constant during the cure and the shrinkage is occurring through reduction of porogen and void volume. However, there are small differences in the matrix volumes between the samples of the same material. In most of the cases, the matrix volume is reduced with increasing curing time, and the effect is stronger for lamp A, which supports directly the proposed mechanism [13] of shrinkage due to SiCH3 removal. The mean volumes (in arbitrary units) of the matrix for the four groups of samples with given material and curing lamps are CVD1A (38.9±1.7), CVD1B (41.0±0.8), CVD2A (60.0±2.0), CVD2B (62.8±1.2). These data quantitatively show stronger reduction of volume of the matrix for lamp A and greater changes from sample to sample (wider dispersion of values) as well.

It should be noted that the porogen removal (creation of pores) is competing with shrinkage of the samples (collapsing the pore volume). We observed reduction of porosity by 0-

2% for the longer curing time compared to shorter curing time for every given combination of material, deposition and curing lamp. Thus, for given moderate curing times, the shrinkage is the stronger effect and leads to collapse of the pores. However, for the full set of samples, the higher shrinkages are observed on samples with higher porosities, as mentioned before.

Ellipsometric porosimetry

The ellipsometric porosimetry gives the information about porosity percentage as well as the pore size distribution (PSD). For the given samples, we observe narrow PSD with the typical FWHM around 1 nm. In the figure 3b, we plotted the modus of the PSD versus porosity. It is observed that the material with higher porosity (less porogen residue) contains larger pores, That can be seen particularly in the behavior of material CVD1, which is deposited with more porogen precursor and therefore the removal (or residue) of porogen plays more important role.

CONCLUSIONS

All the observed facts might be summarized by following interpretation: The materials are deposited with "intrinsic" porosity around 40% for CVD1 and 60% for CVD2, and most of the space is occupied by porogen. During the UV-cure, the porogen is decomposed and significant part of it is removed. The material shrinks mainly through the pore collapse, while some shrinkage is observed for the matrix itself due to the replacement of $SiCH_3$ by SiH. There is also some rearrangement of SiO_2 backbone towards "network" structure. However, some of the porogen material stays in the pore interior leading to effectively smaller pores. The chemical structure of the residues is different from the as-deposited porogen. There is a transition from the hydrocarbon structure (detected as characteristic bands around 2900 cm^{-1} in the FTIR) towards carbon rich material (with aromatic or amorphous arrangement) giving rise to the absorption band in the ultraviolet (around 4 eV), which should be attributed to π-π^* electronic transitions of sp^2 bonded carbon [17], and also to C=C vibration at 1600 cm^{-1} in the infrared. This phenomenon has been already presented [2] for annealed porogen-based low-k's.

The results of our recent research presented in this paper and in [7,8,15,18], show that chemical and physical properties of low-k films can be controlled by wavelength of UV light. The critical threshold is near 190 nm, which was also proven by quantum-chemical calculations. UV light with $\lambda > 200$ nm allows to remove porogen without significant residue formation and also allow to avoid formation of SiH bonds that have higher polarisability in comparison with Si-CH3 bonds and generally more chemically reactive. However, it was found that chemical resistance of low-k materials to HF solutions and NH_3 plasma almost doesn't depends on presence of SiH groups.

ACKNOWLEDGMENTS

It is our pleasure to thank for the help and valuable contribution S.Eslava, D.Shamiryan, G.Beyer (IMEC), H.Sprey, J.Beynet; K.Matsushita, N.Tsuji, S.Kaneko (ASM) and S.Naumov (IOM).

REFERENCES

1. K. Maex, M. R. Baklanov, D. Shamiryan, F. Iacopi, S. H. Brongersma, and Z. S. Yanovitskaya, Journal of Applied Physics **93** (2003) 8793.
2. S. M. Gates, D. A. Neumayer, M. H. Sherwood, A. Grill, X. Wang, and M. Sankarapandian, Journal of Applied Physics **101** (2007) 094103.
3. A. Grill and V. Patel, Journal of Applied Physics **104** (2008) 024113.
4. A. Zenasni, V. Jousseaume, P. Holliger, L. Favennec, O. Gourhant, P. Maury, and G. Gerbaud, Journal of Applied Physics **102** (2007) 094107.
5. N. Kemeling, K. Matsushita, N. Tsuji, K. Kagami, M. Kato, S. Kaneko, H. Sprey, D. de Roest, and N. Kobayashi, Microelectronic Engineering **84** (2007) 2575.
6. F. Iacopi, Y. Travaly, B. Eyckens, C. Waldfried, T. Abell, E. P. Guyer, D. M. Gage, R. H. Dauskardt, T. Sajavaara, K. Houthoofd, P. Grobet, P. Jacobs, and K. Maex, Journal of Applied Physics **99** (2006) 053511.
7. S. Eslava, F. Iacopi, A. M. Urbanowicz, C. E. A. Kirschhock, K. Maex, J. A. Martens, and M. R. Baklanov, Journal of the Electrochemical Society **155** (2008) G231.
8. L. Prager, P.Marsik, J.W. Gerlach, M.R. Baklanov, S. Naumov, L. Pistol, D. Schneider, L. Wennrich, P. Verdonck, M.R. Baklanov, Microelectronic Engineering **85**(2008) 2094.
9. L. Favennec, V. Jousseaume, G. Gerbaud, A. Zenasni, and G. Passemard, Journal of Applied Physics **102** (2007) 064107.
10. J. Humlicek, in: H. Tompkins, E. Irene (Eds.), Handbook of Ellipsometry, William Andrew Publishing, New York, 2005
11. J. Humlicek, Analysis of spectrum line profiles. analysis of spectrum line profiles, FOLIA Fac. Sci. Nat. UP Brunensis, Physica 36 (1984).
12. M. R. Baklanov,K. P. Mogilnikov, V. G. Polovinkin, F. N. Dultsev, J.Vac.Sci.Technol. **B18** (2000) 1385-1391.
13. J. Ushio, T. Ohno, T. Hamada, S. I. Nakao, K. Yoneda, M. Kato, and N. Kobayashi, Japanese Journal of Applied Physics Part 2-Letters & Express Letters **46** (2007) L405.
14. P. Marsik, article in preparation
15. S. Eslava, G. Eymery, P. Marsik, F. Iacopi, C. E. A. Kirschhock, K. Maex, J. A. Martens, and M. R. Baklanov, Journal of the Electrochemical Society **155** (2008) G115.
16. D. E. Aspnes, Thin Solid Films **89** (1982) 249.
17. M. Gioti and S. Logothetidis, Diamond and Related Materials **12** (2003) 957.
18. A. M. Urbanowicz, B. Meshman, D. Schneider, and M. R. Baklanov. phys. stat. sol. (a) 205, No. 4 (2008) 829.